J. FAC. SCI., SHINSHU UNIVERSITY, Vol. 29, No. 1, pp.9-20 1994

Magnetic excitations in antiferromagnetic Bi_2CuO_4

Kazuaki MURAYAMA*, Kazuhiko SAIKAWA and Kazuko MOTIZUKI**

Department of Physics, Faculty of Science, Shinshu University
Matsumoto, Japan

Abstract

Magnetic excitations in the antiferromagnetic Bi_2CuO_4 (T_N=42K) are investigated on the basis of anisotropic exchange interaction between spins of Cu^{2+} ions. We calculate the dispersion curves and evaluate the intensity of the inelastic neutron scattering by spin wave excitations. The results are discussed in connection with observations. Spin contraction at 0K, temperature dependence of the sublattice magnetization and field dependence of the antiferromagnetic resonance frequency are calculated. Furthermore, the effect of spin wave interaction on the spin wave dispersions is investigated in the framework of the random phase approximation.

1 Introduction

The discovery of the high temperature oxide superconductors has led to increasing interest in studies of the physical properties of CuO-based materials. Among the vast group of Cu-based materials, Bi_2CuO_4 attracts special attention because of its interesting crystal structure and magnetic properties. Bi_2CuO_4 belongs to the tetragonal space group P4/ncc. In this compound CuO_4 units, one of which consists of a square of O ions and a Cu^{2+} ion at the center, are stacked along the c-axis in a staggered manner, but in the c-plane two adjacent CuO_4 units are separated with each other by an intervened Bi cation. Only Cu^{2+} cations are illustrated in Fig. 1 . The antiferromagnetic 3-dimensional long range order was confirmed below T_N=42K by neutron diffraction measurements.[1] As shown in Fig. 1 magnetic moments align ferromagnetically along the c-axis and antiferromagnetically between corner sites and inter sites. The easy direction lies in the c-plane.

Up to now this compound has been intensively studied by various experiments. For single crystal of Bi_2CuO_4 , Ohta *et al.*[2] observed paramagnetic and antiferromagnetic resonances and analyzed the observed results by using the molecular field model based

* Present address : Faculty of Technology, Gumma University Kiriu 376, Japan
** Present address : Department of Physics, Faculty of Science, Okayama University of Science Okayama 700, Japan

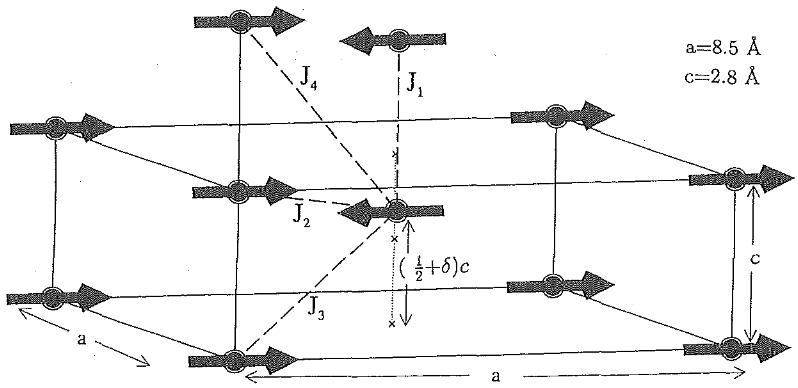

Fig. 1 : Arrangement of Cu^{2+} spins and the parameters of the exchange interactions used in the present calculation are shown together with the lattice parameters.

on the anisotropic exchange Hamiltonian. With use of inelastic neutron scattering measurements the spin wave excitation of this compound has been investigated recently by two different groups. As for their results there is some controversy : Aïn *et al.*[3] reported the existence of a single doubly degenerate dispersion branch, while Furrer *et al.*[4] found two branches with finite energy gaps at $\boldsymbol{q}=0$.

In the present paper, first the spin wave dispersions are studied theoretically on the basis of the anisotropic exchange interactions between spins of Cu^{2+} ions. Spin contraction at 0K is estimated and temperature dependence of the sublattice magnetization and field dependence of the antiferromagnetic resonance frequency are calculated. Next the intensity of the inelastic neutron scattering due to the spin waves is calculated and the results are compared with observations. Finally the effect of spin wave interaction is investigated by taking account of fourth order terms in the exchange Hamiltonian with respect to magnon operators.

2 Spin wave dispersion

In the system of Cu^{2+} ions the anisotropy energy of the one-ion type arising from the crystalline electric field vanishes completely. Therefore, the anisotropic exchange interaction plays an important role as the origin of the anisotropy energy. For the antiferromagnetic Bi_2CuO_4 we adopt two sublattice (1 and 2) model and assume the anisotropic exchange Hamiltonian as follows :

$$
\begin{aligned}
H=&-2\sum_{(i,i')pair}[J_{11ii'}S^x_{1i}S^x_{1i'}+(J_{11ii'}+D_{11ii'})S^y_{1i}S^y_{1i'}+J_{11ii'}S^z_{1i}S^z_{1i'}]\\
&-2\sum_{(j,j')pair}[J_{22jj'}S^x_{2j}S^x_{2j'}+(J_{22jj'}+D_{22jj'})S^y_{2j}S^y_{2j'}+J_{22jj'}S^z_{2j}S^z_{2j'}]\\
&-2\sum_{i,j}[J_{12ij}S^x_{1i}S^x_{2j}+(J_{12ij}+D_{12ij})S^y_{1i}S^y_{2j}+J_{12ij}S^z_{1i}S^z_{2j}], \qquad (1)
\end{aligned}
$$

where i and i' denote atomic sites in the sublattice 1 and j and j' stand for those in the sublattice 2. The notation $J_{11ii'}$ ($J_{22jj'}$) represents the isotropic part of the coefficient of the exchange interaction between spins in the sublattice 1(2) and $D_{11ii'}$ ($D_{22jj'}$) represents the remaining anisotropic part of the exchange interaction coefficient. The y-direction is taken to be along the c-axis and the z-direction is parallel to the spin direction in the c-plane. Furthermore, S_{1i}^x, for instance, stands for the x component of the spin operator at the i-th site in the sublattice 1.

The Hamiltonian given by eq. (1) can be written in terms of the spin deviation operators, a_i, $a_i^\dagger$, b_j and $b_j^\dagger$ defined by

$$\begin{aligned} S_{1i}^z &= S - a_i^\dagger a_i \\ S_{1i}^+ &= S_{1i}^x + iS_{1i}^y = \sqrt{2S}\left(1 - \frac{a_i^\dagger a_i}{2S}\right)^{1/2} a_i \\ S_{1i}^- &= S_{1i}^x - iS_{1i}^y = \sqrt{2S}\, a_i^\dagger \left(1 - \frac{a_i^\dagger a_i}{2S}\right)^{1/2} \end{aligned} \tag{2}$$

and

$$\begin{aligned} S_{2j}^z &= -S + b_j^\dagger b_j \\ S_{2j}^+ &= S_{2j}^x + iS_{2j}^y = \sqrt{2S}\, b_j^\dagger \left(1 - \frac{b_j^\dagger b_j}{2S}\right)^{1/2} \\ S_{2j}^- &= S_{2j}^x - iS_{2j}^y = \sqrt{2S}\left(1 - \frac{b_j^\dagger b_j}{2S}\right)^{1/2} b_j. \end{aligned} \tag{3}$$

We perform Fourier transformations:

$$\begin{aligned} a_q &= \frac{1}{\sqrt{N}} \sum_{i\in 1} a_i \exp(-i\boldsymbol{q}\cdot\boldsymbol{r}_i) \qquad & a_q^\dagger &= \frac{1}{\sqrt{N}} \sum_{i\in 1} a_i^\dagger \exp(i\boldsymbol{q}\cdot\boldsymbol{r}_i) \\ b_q &= \frac{1}{\sqrt{N}} \sum_{j\in 2} b_j \exp(-i\boldsymbol{q}\cdot\boldsymbol{r}_j) \qquad & b_q^\dagger &= \frac{1}{\sqrt{N}} \sum_{j\in 2} b_j^\dagger \exp(i\boldsymbol{q}\cdot\boldsymbol{r}_j) \end{aligned} \tag{4}$$

and

$$\begin{aligned} J_{11}(\boldsymbol{q}) &= \sum_{i\in 1, i'\in 1} J_{11ii'} \exp[-i\boldsymbol{q}\cdot(\boldsymbol{r}_i - \boldsymbol{r}_{i'})] = J_{22}(\boldsymbol{q}) \\ J_{12}(\boldsymbol{q}) &= \sum_{i\in 1, j\in 2} J_{12ij} \exp[-i\boldsymbol{q}\cdot(\boldsymbol{r}_i - \boldsymbol{r}_j)], \end{aligned} \tag{5}$$

where N is the number of spins per sublattice, and $\boldsymbol{r}_i$ or $\boldsymbol{r}_{i'}$ denotes the position vector of the spin i or i' in the sublattice 1 and $\boldsymbol{r}_j$ denotes the position vector of the spin j in the sublattice 2. The Fourier transforms $D_{11}(\boldsymbol{q}) = D_{22}(\boldsymbol{q})$ and $D_{12}(\boldsymbol{q})$ are similarly defined. Then the Hamiltonian (1) can be written as

$$\begin{aligned} H = &-\frac{1}{2}(4S^2)N[J_{11}(0) - J_{12}(0)] \\ &-\frac{2S}{4}\sum_{\boldsymbol{q}}\{[4J_{11}(\boldsymbol{q}) + 2D_{11}(\boldsymbol{q}) - 4J_{11}(0) + 4J_{12}(0)]a_q^\dagger a_q \\ &-D_{11}(\boldsymbol{q})\, a_q\, a_{-q} - D_{11}(\boldsymbol{q})\, a_q^\dagger a_{-q}^\dagger \end{aligned}$$

$$+[4J_{11}(\boldsymbol{q})+2D_{11}(\boldsymbol{q})-4J_{11}(0)+4J_{12}(0)]b_q^\dagger b_q$$
$$-D_{11}(\boldsymbol{q})b_q b_{-q}-D_{11}(\boldsymbol{q})b_q^\dagger b_{-q}^\dagger$$
$$+[4J_{12}(\boldsymbol{q})+2D_{12}(\boldsymbol{q})]a_q^\dagger b_{-q}^\dagger+[4J_{12}(-\boldsymbol{q})+2D_{12}(-\boldsymbol{q})]a_q b_{-q}$$
$$-2D_{12}(\boldsymbol{q})a_q^\dagger b_q-2D_{12}(-\boldsymbol{q})a_q b_{-q}^\dagger\}. \quad (6)$$

In order to diagonalize the Hamiltonian given by eq. (6) we make transformation as

$$\xi_q=\mu_q a_q+\nu_q a_{-q}^\dagger+\rho_q b_q+\lambda_q b_{-q}^\dagger \quad (7)$$

which satisfies the equation

$$[\xi_q, H]=\hbar\omega_q\xi_q. \quad (8)$$

Finally, we obtain two kinds of eigenvalue:

$$\hbar\omega_q=\left[\varepsilon_q^2-|A_q|^2+|B_q|^2\pm\sqrt{4|B_q|^2(\varepsilon_q^2-|A_q|^2)+(A_qB_q^*+A_q^*B_q)^2}\right]^{1/2} \quad (9)$$

where

$$\varepsilon_q=\frac{1}{4}\{-[D_{11}(\boldsymbol{q})+D_{11}(-\boldsymbol{q})]^2$$
$$+[2J_{11}(\boldsymbol{q})+2J_{11}(-\boldsymbol{q})+D_{11}(\boldsymbol{q})+D_{11}(-\boldsymbol{q})-4J_{11}(0)+4J_{12}(0)]^2\}^{1/2}$$
$$A_q=-\frac{1}{2}\{[2J_{12}(\boldsymbol{q})+D_{12}(\boldsymbol{q})](\cosh^2\theta_q+\sinh^2\theta_q)+2D_{12}(\boldsymbol{q})\cosh\theta_q\sinh\theta_q\} \quad (10)$$
$$B_q=-\frac{1}{2}\{-D_{12}(\boldsymbol{q})(\cosh^2\theta_q+\sinh^2\theta_q)-2[2J_{12}(\boldsymbol{q})+D_{12}(\boldsymbol{q})]\cosh\theta_q\sinh\theta_q\}$$

with

$$\tanh\theta_q=\frac{1}{4}[D_{11}(\boldsymbol{q})+D_{11}(-\boldsymbol{q})]\times\{\varepsilon_q-\frac{1}{4}[2J_{11}(\boldsymbol{q})+2J_{11}(-\boldsymbol{q})+$$
$$+D_{11}(\boldsymbol{q})+D_{11}(-\boldsymbol{q})-4J_{11}(0)+4J_{12}(0)]\}^{-1}. \quad (11)$$

The Hamiltonian (6) has thus been diagonalized in the following form:

$$H=\sum_q[\hbar\omega_q^{AC}(\xi_q^{AC})^\dagger\xi_q^{AC}+\hbar\omega_q^{OP}(\xi_q^{OP})^\dagger\xi_q^{OP}]+\mathrm{const}, \quad (12)$$

where $\hbar\omega_q^{AC}$ corresponds to the eigenvalue with $-$ sign of eq. (9) and $\hbar\omega_q^{OP}$ to that with $+$ sign of eq. (9). We call the spin wave branch for $\hbar\omega_q^{AC}$ as the acoustical branch and that for $\hbar\omega_q^{OP}$ as the optical branch, because at $\boldsymbol{q}=0$ $\hbar\omega_q^{AC}$ becomes zero and $\hbar\omega_q^{OP}$ has a finite value. We consider one kind of intra-sublattice exchange interaction and three kinds of inter-sublattice exchange interactions as shown in Fig. 1. Their coefficients are denoted as J_1, J_2, J_3 and J_4 for the isotropic part and D_1, D_2, D_3 and D_4 for the anisotropic part. In terms of these coefficients the Fourier transforms of the exchange interactions defined by eq. (5) are thus given by

$$J_{11}(\boldsymbol{q})=2J_1\cos(\boldsymbol{q}\cdot\boldsymbol{c}),$$
$$D_{11}(\boldsymbol{q})=2D_1\cos(\boldsymbol{q}\cdot\boldsymbol{c}),$$

$$J_{12}(\boldsymbol{q})=$$
$$4\cos(\frac{\boldsymbol{q}\cdot\boldsymbol{a}}{2})\cos(\frac{\boldsymbol{q}\cdot\boldsymbol{b}}{2})\exp(i\delta\boldsymbol{q}\cdot\boldsymbol{c})[J_2+J_3\exp(-i\boldsymbol{q}\cdot\boldsymbol{c})+J_4\exp(i\boldsymbol{q}\cdot\boldsymbol{c})],$$

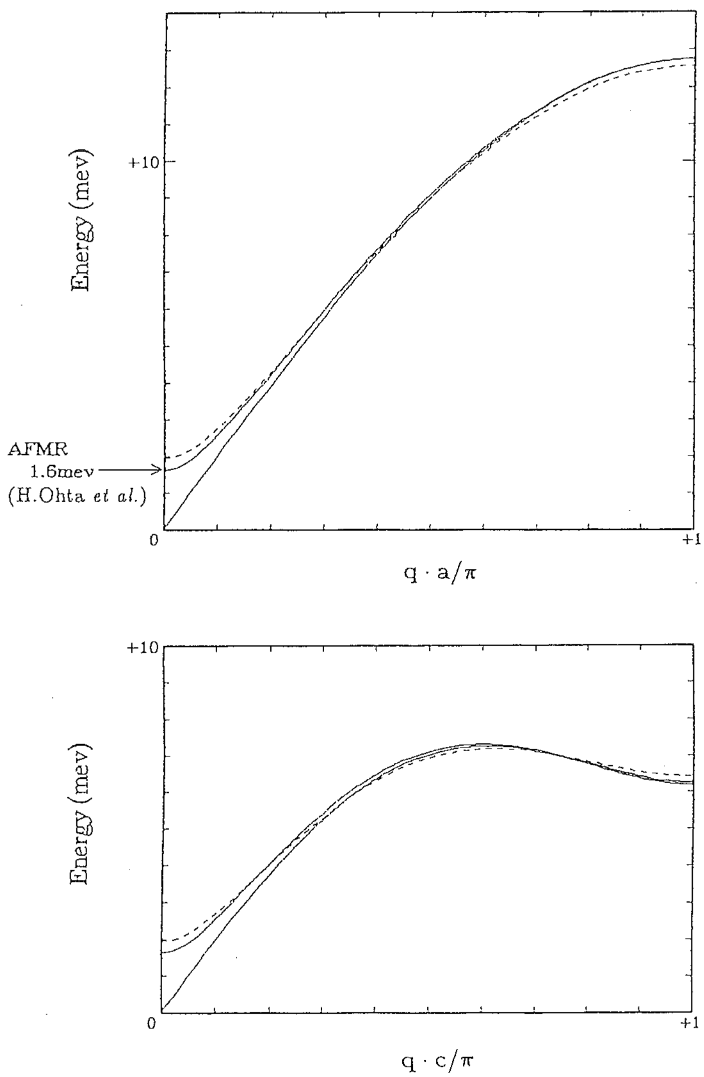

Fig. 2 : Spin wave dispersion curves along the [100] and [001] directions. Solid curves are the calculated results by the free spin wave approximation. Dashed curves represent the observed ones.[3)]

$$D_{12}(\boldsymbol{q})=4\cos(\frac{\boldsymbol{q}\cdot\boldsymbol{a}}{2})\cos(\frac{\boldsymbol{q}\cdot\boldsymbol{b}}{2})\exp(i\delta\boldsymbol{q}\cdot\boldsymbol{c})\times$$
$$\times[D_2+D_3\exp(-i\boldsymbol{q}\cdot\boldsymbol{c})+D_4\exp(i\boldsymbol{q}\cdot\boldsymbol{c})], \quad (13)$$

where $\boldsymbol{a}$, $\boldsymbol{b}$ and $\boldsymbol{c}$ are the lattice vectors characterizing the crystal structure, $\boldsymbol{a}$ and $\boldsymbol{b}$ lying in the c-plane. The parameter δ is defined in Fig. 1 . These values are determined so as to reproduce the observed antiferromagnetic resonance frequency[2] and to fit the optical spin wave dispersion curves calculated along the [001] and [100] directions with those observed by neutron inelastic scattering.[3] We have

$$J_1=-0.84\text{mev} \qquad D_1=-9\times10^{-3}\text{mev}$$
$$J_2=-0.72 \qquad D_2=14\times10^{-3}$$
$$J_3=-0.23 \qquad D_3=0$$
$$J_4=-2.23 \qquad D_4=7\times10^{-3}$$

The calculated spin wave dispersion curves are shown in Fig. 2 together with the observed ones.

In the spin wave approximation the thermal average of each spin is given by the following expression :

$$<S^z>=S-\frac{1}{N}\sum_i<a_i^\dagger a_i>$$
$$=S-\frac{1}{N}\sum_q\{[|\mu_q^{AC}|^2+|\nu_q^{AC}|^2]<(\xi_q^{AC})^\dagger\xi_q^{AC}>$$
$$+[|\mu_q^{OP}|^2+|\nu_q^{OP}|^2]<(\xi_q^{OP})^\dagger\xi_q^{OP}>$$
$$+|\nu_q^{AC}|^2+|\nu_q^{OP}|^2\}. \quad (14)$$

The last term of eq. (14) represents the spin contraction at $T=0$K. By using the results of spin wave dispersion we have calculated $<S^z>$ as a function of temperature. The result is shown in Fig. 3 . At $T=0$K, $<S^z>/S$ is evaluated to be 85%. This value is in good agreement with the value of 84% observed by Yamada *et al.*[1], but is larger than the value of 63% observed by Aïn *et al.*[3]

Next we study the field effect on the spin wave energy. In the case of the external field applied along the spin direction z, the Zeeman interaction is expressed as

$$H^{\parallel}_{\text{Zeeman}}=\sum_q h^z(a_q^\dagger a_q-b_q^\dagger b_q), \quad (15)$$

where

$$h^z=-g\mu_B\text{H},$$

H being the applied external field. In this case, the total Hamiltonian $H+H^{\parallel}_{\text{Zeeman}}$ can be diagonalized and the spin wave energy is obtained as

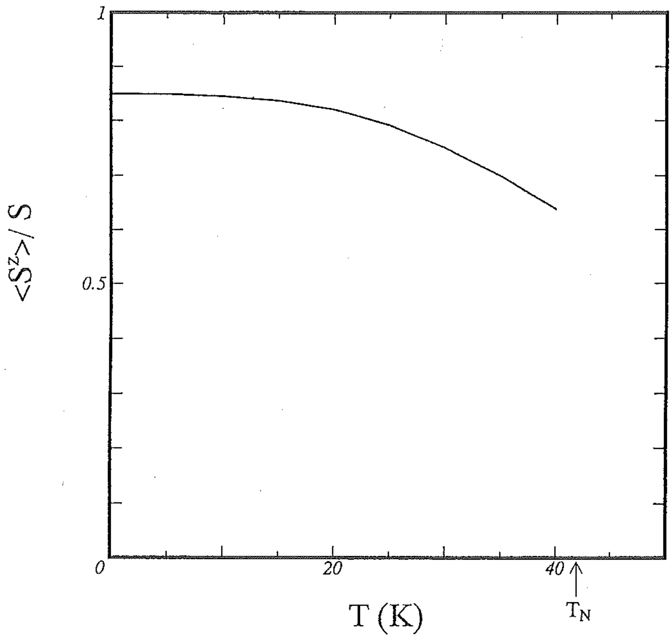

Fig. 3 : Thermal average of a spin as a function of temperature calculated with the free spin wave approximation.

$$\left(\frac{\hbar\omega_k}{2S}\right)^2=\frac{(\varepsilon_k^a)^2+(\varepsilon_k^b)^2}{2}-|A_k|^2+|B_k|^2$$
$$\pm\{4[(\frac{\varepsilon_k^a+\varepsilon_k^b}{2})^2-|A_k|^2][(\frac{\varepsilon_k^a+\varepsilon_k^b}{2})^2+|B_k|^2]+(A_kB_k^*+A_k^*B_k)^2\}^{1/2} \qquad (16)$$

where

$$\varepsilon_q^a=\frac{1}{4}\{[2J_{11}(\boldsymbol{q})+2J_{11}(-\boldsymbol{q})+D_{11}(\boldsymbol{q})+D_{11}(-\boldsymbol{q})$$
$$-4J_{11}(0)+4J_{12}(0)-4h^z]^2-[D_{11}(\boldsymbol{q})+D_{11}(-\boldsymbol{q})]^2\}^{1/2}$$
$$\varepsilon_q^b=\frac{1}{4}\{[2J_{11}(\boldsymbol{q})+2J_{11}(-\boldsymbol{q})+D_{11}(\boldsymbol{q})+D_{11}(-\boldsymbol{q})$$
$$-4J_{11}(0)+4J_{12}(0)+4h^z]^2-[D_{11}(\boldsymbol{q})+D_{11}(-\boldsymbol{q})]^2\}^{1/2}, \qquad (17)$$

and A_q and B_q are given in the forms of eqs. (10) with replacement of $\cosh^2\theta_q$, $\sinh^2\theta_q$ and $2\sinh\theta_q\cosh\theta_q$ by $\cosh\theta_q^a\cosh\theta_q^b$, $\sinh\theta_q^a\sinh\theta_q^b$ and $\sinh\theta_q^a\cosh\theta_q^b+\sinh\theta_q^b\cosh\theta_q^a$ respectively. The angles θ_q^a and θ_q^b are defined by

$$\tanh\theta_q^a=\frac{1}{4}[D_{11}(\boldsymbol{q})+D_{11}(-\boldsymbol{q})]\times\{\varepsilon_q^a-\frac{1}{4}[2J_{11}(\boldsymbol{q})$$
$$+2J_{11}(-\boldsymbol{q})+D_{11}(\boldsymbol{q})+D_{11}(-\boldsymbol{q})-4J_{11}(0)+4J_{12}(0)-4h^z]\}^{-1},$$
$$\tanh\theta_q^b=\frac{1}{4}[D_{11}(\boldsymbol{q})+D_{11}(-\boldsymbol{q})]\times\{\varepsilon_q^b-\frac{1}{4}[2J_{11}(\boldsymbol{q})$$

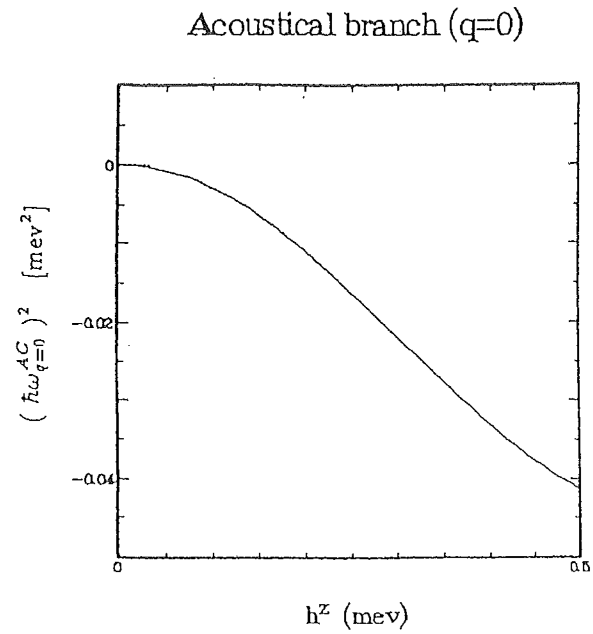

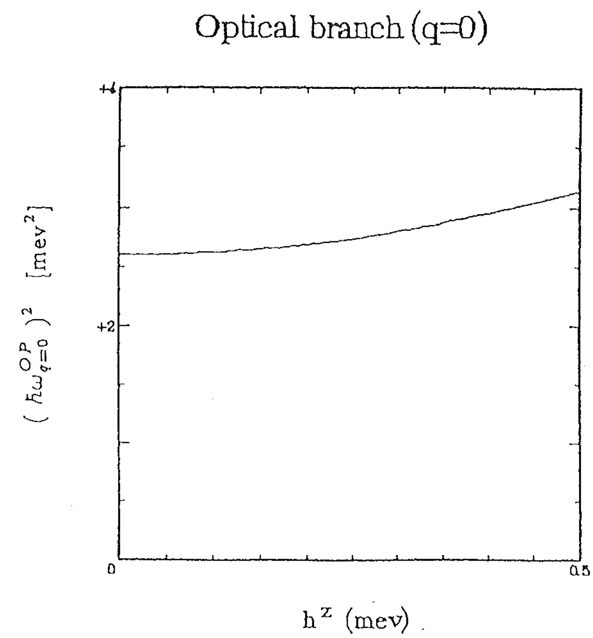

Fig. 4 : Field dependence of the spin wave energy at $\boldsymbol{q} = 0$ in the case of the external magnetic field applied along the spin direction (z-axis) are shown for the acoustic and optical branches.

$$+2J_{11}(-\boldsymbol{q})+D_{11}(\boldsymbol{q})+D_{11}(-\boldsymbol{q})-4J_{11}(0)+4J_{12}(0)+4h^z]\}^{-1}. \tag{18}$$

For $\boldsymbol{q} = 0$, we have found that the spin wave energy of the optical branch increases quadratically with increasing external field as shown in Fig. 4 . On the other hand, the spin wave energy of acoustical branch becomes imaginary. This fact is understood in the following way. The normal mode of the acoustical branch at $\boldsymbol{q} = 0$ corresponds to the uniform mode in the c-plane, because in the present calculation we have neglected anisotropy energy in the c-plane. Therefore spin flop occurs easily due to the applied field parallel to the spin direction. If a small anisotropy energy is introduced in the c -plane, the acoustical branch will have a finite energy gap at $\boldsymbol{q} = 0$. This gap will decrease with increasing field and vanish at spin flop field which was observed.

When the external field is applied perpendicular to the spin direction, the Zeeman interaction is given by

$$H^{\perp}_{\text{Zeeman}} = -h^x(a_0 + a_0^\dagger + b_0 + b_0^\dagger). \tag{19}$$

This interaction has an effect only for $\boldsymbol{q} = 0$. The total Hamiltonian, eq. (6) + Zeeman interaction, can be diagolized for $\boldsymbol{q} = 0$ as follows:

$$H + H^{\perp}_{\text{Zeeman}} = \hbar\omega_0^{AC}(\xi_0^{AC})^\dagger(h^x)\xi_0^{AC}(h^x) + \hbar\omega_0^{OP}(\xi_0^{OP})^\dagger(h^x)\xi_0^{OP}(h^x) + \text{const}, \tag{20}$$

where

$$\xi_0^{AC}(h^x) = \xi_0^{AC} - \frac{h^x P}{\hbar\omega_0^{AC}}$$
$$\xi_0^{OP}(h^x) = \xi_0^{OP} - \frac{h^x Q}{\hbar\omega_0^{OP}}. \tag{21}$$

Furthermore, P and Q in eq. (21) are given by

$$P = \mu_0^{AC} - \nu_0^{AC*} + \rho_0^{AC} - \lambda_0^{AC*}$$
$$Q = \mu_0^{OP} - \nu_0^{OP*} + \rho_0^{OP} - \lambda_0^{OP*}.$$

Therefore the spin wave energy at $\boldsymbol{q} = 0$ does not depend on the applied field in this case. In order to discuss the field effect we must take into account fourth order terms in the Hamiltonian with respect to the magnon operators.

3 Intensity of neutron scattering by magnetic excitations

The differential cross-section of neutron scattering by magnetic excitations can be written in terms of the correlation function of spin moment operators in the form

$$\frac{d^2\sigma}{d\Omega dE} \propto \sum_{\alpha,\beta}(\delta_{\alpha\beta} - e_\alpha e_\beta) \times \int_{-\infty}^{\infty} dt\ \exp(iEt/\hbar)\sum_{i,j}\exp(i\vec{K}\cdot\vec{R}_{i,j}) < S_{i\alpha}(0)S_{j\beta}(t) >, \tag{22}$$

where $\vec{e}\equiv\vec{K}/|\vec{K}|$ ($\vec{K}$: a scattering vector), α and β denote x, y, z (z: the spin direction), and $<\ >$ represents the thermal average.

We have calculated the correlation function $<S_{i\alpha}(0)S_{j\beta}(t)>$ in the framework of the spin wave approximation. At zero temperature, the scattering intensity due to emissions of magnons of the acoustical branch, I_{AC}, and that of the optical branch, I_{OP}, are obtained as follows:

$$\begin{aligned} I_{AC}\infty k_f[&|(2K^2-K^+K^-)(-\nu_{\tilde{K}}^{AC*}+e^{-iG_K\cdot\Delta}\rho_{\tilde{K}}^{AC*})-(K^+)^2(\mu_{\tilde{K}}^{AC*}-e^{-iG_K\cdot\Delta}\lambda_{\tilde{K}}^{AC*})|^2 \\ &+|(2K^2-K^+K^-)(\mu_{\tilde{K}}^{AC*}-e^{-iG_K\cdot\Delta}\lambda_{\tilde{K}}^{AC*})-(K^-)^2(-\nu_{\tilde{K}}^{AC*}+e^{-iG_K\cdot\Delta}\rho_{\tilde{K}}^{AC*})|^2 \\ &+2(K^z)^2|K^-(-\nu_{\tilde{K}}^{AC*}+e^{-iG_K\cdot\Delta}\rho_{\tilde{K}}^{AC*})+K^+(\mu_{\tilde{K}}^{AC*}-e^{-iG_K\cdot\Delta}\lambda_{\tilde{K}}^{AC*})|^2] \end{aligned}$$

$$\begin{aligned} I_{OP}\infty k_f[&|(2K^2-K^+K^-)(-\nu_{\tilde{K}}^{QP*}+e^{-iG_K\cdot\Delta}\rho_{\tilde{K}}^{QP*})-(K^+)^2(\mu_{\tilde{K}}^{QP*}-e^{-iG_K\cdot\Delta}\lambda_{\tilde{K}}^{QP*})|^2 \\ &+|(2K^2-K^+K^-)(\mu_{\tilde{K}}^{QP*}-e^{-iG_K\cdot\Delta}\lambda_{\tilde{K}}^{QP*})-(K^-)^2(-\nu_{\tilde{K}}^{QP*}+e^{-iG_K\cdot\Delta}\rho_{\tilde{K}}^{QP*})|^2 \\ &+2(K^z)^2|K^-(-\nu_{\tilde{K}}^{QP*}+e^{-iG_K\cdot\Delta}\rho_{\tilde{K}}^{QP*})+K^+(\mu_{\tilde{K}}^{QP*}-e^{-iG_K\cdot\Delta}\lambda_{\tilde{K}}^{QP*})|^2], \end{aligned} \quad (23)$$

where $K^{\pm}\equiv K^x\pm iK_y$, and $\mu_{\tilde{K}}^{AC}$, $\nu_{\tilde{K}}^{AC}$, $\rho_{\tilde{K}}^{AC}$, $\lambda_{\tilde{K}}^{AC}$ represent the coefficients of the transformation defined by eq. (7) in § 2 for the acoustical branch and $\mu_{\tilde{K}}^{QP}$ etc, represent those for the optical branch. Here for a given scattering vector $\vec{K}$, we have defined the reduced vector $\tilde{\boldsymbol{K}}=\vec{K}-\boldsymbol{G}_K$ in the first Brillouin zone with the appropriate reciprocal lattice vector $\boldsymbol{G}_K$. The notation $\boldsymbol{\Delta}$ stands for the position vector of an atom belonging to the sublattice 2 relative to the atom belonging to the sublattice 1 in the same unit cell, namely, $\boldsymbol{\Delta}=\frac{1}{2}\boldsymbol{a}+\frac{1}{2}\boldsymbol{b}+\delta\boldsymbol{c}$, where $\boldsymbol{a},\boldsymbol{b}$ and $\boldsymbol{c}$ are the lattice vectors.

We have calculated the ratio of I_{AC} to I_{OP} for the three kinds of scattering vectors, (0, 0, 1/20), (1, 0, 1/20), (0, 1, 1/20) and the results are shown in Table 1. It should be noted here that the scattering vectors (1, 0, 1/20) etc. are described by using the coordinate axes which are referred to the crystal axes a, b and c. The relation between a, b, c and x, y, z axes is as follows: a // z, b // x, c // y. As seen in the table, for the measurement at (1, 0, 1/20) both the acoustical and optical branches are observable, but for the measurement at (0, 1, 1/20) it is difficult to observe the acoustical branch.

Table 1 : The calculated intensity ratio of I_{AC} to I_{OP} for the three scattering vectors.

Scattering vector	Intensity ratio I_{AC}/I_{OP}
(0,0,1/20)	3.0
(1,0,1/20)	1.3
(0,1,1/20)	4.1×10^{-3}

4 Effect of magnon-magnon interaction

In the case of $S = 1/2$ like Cu^{2+} ions, the magnon-magnon interaction, which arises from higher-order terms in the Hamiltonian expanded by magnon operators, is important because the Holstein - Primakoff method is based on the expansion of

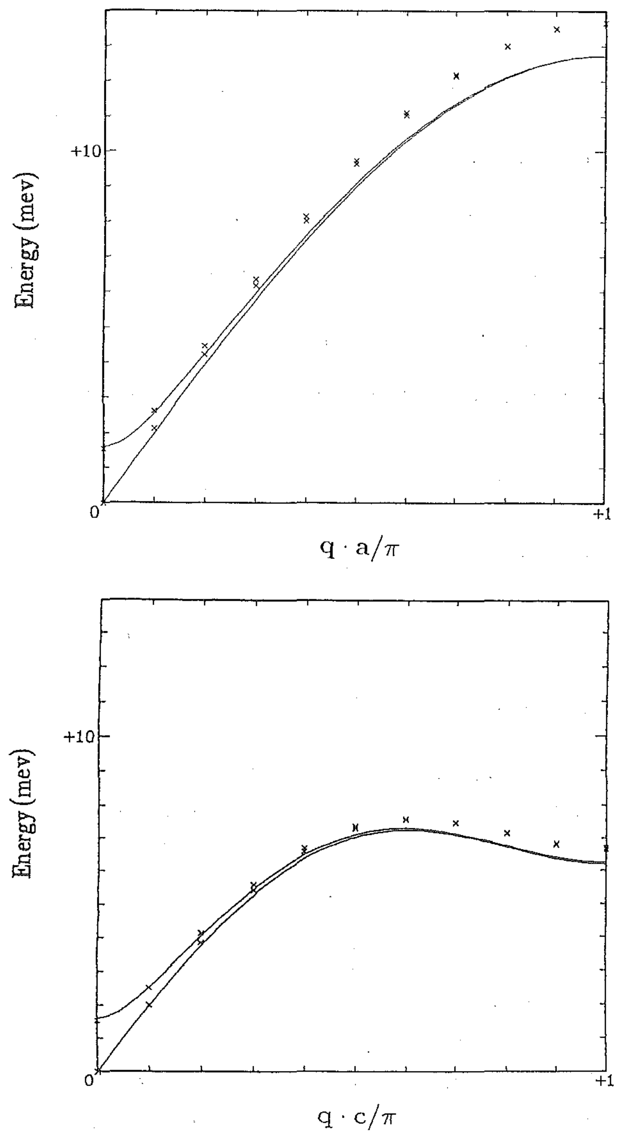

Fig. 5 : Cross points denote the spin wave energies calculated at 0K by taking account of the spin wave interaction. For comparison, spin wave dispersions calculated by the free spin wave approximation are shown by solid curves.

spin operators in powers of $1/S$. In the framework of the random phase approximation, the fourth-order terms with respect to magnon operators a_q and b_q of the Hamiltonian given by eq. (6) is obtained as

$$H_4^{\mathrm{RPA}}=\frac{1}{4}\sum_{\boldsymbol{q}}\{[(8J_{11}(\boldsymbol{q})-8J_{11}(0)+8J_{12}(0))\varDelta S$$

$$+\frac{1}{N}\sum_{\boldsymbol{k}}((8J_{11}(\boldsymbol{k})-8J_{11}(\boldsymbol{k}-\boldsymbol{q}))<a_k^\dagger a_k>$$

$$+4J_{12}(-\boldsymbol{k})<a_k b_{-k}>+4J_{12}(\boldsymbol{k})<a_k^\dagger b_{-k}^\dagger>)]a_q^\dagger a_q$$

$$+\frac{1}{N}\sum_{\boldsymbol{k}}[(2J_{11}(\boldsymbol{q})+2J_{11}(\boldsymbol{k})-4J_{11}(\boldsymbol{k}-\boldsymbol{q}))<a_k^\dagger a_{-k}^\dagger>+2J_{12}(\boldsymbol{k})<a_k^\dagger b_k>]a_q a_{-q}$$

$$+\frac{1}{N}\sum_{\boldsymbol{k}}[(2J_{11}(\boldsymbol{q})+2J_{11}(\boldsymbol{k})-4J_{11}(\boldsymbol{k}-\boldsymbol{q}))<a_k a_{-k}>+2J_{12}(\boldsymbol{k})<a_k b_k^\dagger>]a_q^\dagger a_{-q}^\dagger$$

+ [terms obtained from the foregoing expressions by interchanging the roles of a and b]

$$+[8J_{12}(-\boldsymbol{q})\varDelta S+\frac{1}{N}\sum_{\boldsymbol{k}}8J_{12}(\boldsymbol{k}-\boldsymbol{q})<a_k^\dagger b_{-k}^\dagger>]a_q b_{-q}$$

$$+[8J_{12}(\boldsymbol{q})\varDelta S+\frac{1}{N}\sum_{\boldsymbol{k}}8J_{12}(\boldsymbol{q}-\boldsymbol{k})<a_k b_{-k}>]a_q^\dagger b_{-q}^\dagger$$

$$+\frac{1}{N}\sum_{\boldsymbol{k}}[(2J_{12}(-\boldsymbol{q})(<a_k^\dagger a_{-k}^\dagger>+<b_k b_{-k}>)+8J_{12}(\boldsymbol{k}-\boldsymbol{q})<a_k^\dagger b_k>]a_q b_q^\dagger$$

$$+\frac{1}{N}\sum_{\boldsymbol{k}}[(2J_{12}(\boldsymbol{q})(<a_k a_{-k}>+<b_k^\dagger b_{-k}^\dagger>)+8J_{12}(\boldsymbol{q}-\boldsymbol{k})<a_k b_k^\dagger>]a_q^\dagger b_q\}, \quad (24)$$

where $\varDelta S$ represents the spin contraction S-$<S^z>$ at 0K expressed by the second term of eq. (14) and only the isotropic part of exchange interaction is taken into consideration since the anisotropic part is very small as shown in § 2. The total Hamiltonian, the sum of eq. (6) and H_4^{RPA}, can be diagonalized by the method described in § 2.

The spin wave energies at 0K calculated by including magnon-magnon interaction are shown in Fig. 5 . The energies are a little bit larger than those, which follow the free spin wave theory, due to the effect of the zero-point motion of spins. This tendency is remarkable near the zone boundary. As for the temperature dependence of the spin wave energy it is necessary to calculate the thermal averages appearing in H_4^{RPA} self-consistently. This is a complicate task and remains as a future problem.

Reference

[1] K. Yamada, K. Takeda, S. Hosoya, Y. Watanabe, Y. Endoh, N. Tomonaga, T. Suzuki, T. Ishigaki, T. Kamiyama, H. Asano and F. Izumi : J. Phys. Soc. Jpn **60** (1991) 2406.

[2] H. Ohta, K. Yoshida, T. Matsuya, T. Namba, M. Motokawa, K. Yamada, Y. Endoh and S. Hosoya : J. Phys. Soc. Jpn **61** (1992) 2921.

[3] M. Aïn, G. Dhalenne, O. Guiselin, B. Hennion and A. Revcolevschi : Phys. Rev. B **47** (1993) 8167.

[4] A. Furrer, P. Fisher, B. Roessli, G. Petrakovskii, K. Sablina, V. Valkov and B. Fedoseev : Solid State Commun. **82** (1992) 443.